A novel unified model for laminated composite beams

Trung-Kien Nguyen[a,*], Ba-Duy Nguyen[a,b], Thuc P. Vo[c], Huu-Tai Thai[d]

[a] *Faculty of Civil Engineering, Ho Chi Minh City University of Technology and Education, 1 Vo Van Ngan Street, Thu Duc District, Ho Chi Minh City, Viet Nam*

[b] *Faculty of Civil Engineering, Thu Dau Mot University, 6 Tran Van On Street, Phu Hoa District, Thu Dau Mot City, Binh Duong Province, Viet Nam*

[c] *School of Engineering and Mathematical Sciences, La Trobe University, Bundoora, VIC 3086, Australia*

[d] *Department of Infrastructure Engineering, The University of Melbourne, Parkville VIC 3010, Australia*

Abstract

Based on fundamental equations of the elasticity theory, a novel unified beam model is developed for laminated composite beams. In this model, the displacement field is selected in a unified form which can be recovered to that of existing shear deformation beam theories available in the literature. Based on Lagrange's equations, the governing equations of the present theory are derived. They are then solved for deflections, stresses, natural frequencies and critical buckling loads of composite beams under different boundary conditions and lay-ups by using the Ritz approach with novel hybrid trigonometric functions. Various examples are also presented to verify the accuracy and generalization of the present theory, as well as investigate the influences of fibre angle on the behaviour of composite beams under different boundary conditions and lay-ups.

Keywords: Shear deformation beam theory; Laminated composite beam; Vibration; Bending; Buckling

1. Introduction

Laminated composite materials are commonly used in spacecraft, aircraft, mechanical engineering, construction and other different engineering fields due to their excellent mechanical properties including high strength, high stiffness and lightweight. The widespread applications of these structures led to the development of different computational models to predict their behaviours.

A general review of theories to analyse the laminated composite beams can be found in the previous works [1–5]. Generally, their behaviours can be captured based on either 2D beam theories or 3D theory of elasticity. The first approach is more popular due to its simplicity, whilst the second one is complicated to implement although it can analyse exactly response. Based on the first method, a

*Corresponding author

Email address: kiennt@hcmute.edu.vn (Trung-Kien Nguyen)

huge number of shear deformation models have been developed for composite beams. The simplest one is the first-order shear deformation beam theory (FSBT) which requires a shear correction factor to compensate for the inadequate distribution of shear stress. The higher-order shear deformation beam theory (HSBT) with higher-order variations of axial displacement gives slightly improved predictions compared with FSBT. However, it involves more number of unknowns and thus is more complicated than FSBT. Another shear deformation beam theory developed based on the first approach is quasi-3D theory where both axial and transverse displacements are approximated as high-order variations through the beam thickness. Therefore, quasi-3D theory can predict the behaviour of composite beams more accurately than HSBT. However, quasi-3D theory is more complicated than HSBT because it involves more numbers of unknowns. Both HSBT and quasi-3D theory do not require the shear correction factor. However, their accuracy strictly depends on a choice of shear functions. The development of shear functions for these theories is therefore an interesting topic that has attracted many researches with different approaches. Various types of shear functions have been developed for composite plates such as polynomial ([6–10]), trigonometric ([11–17]), exponential ([18]), hyperbolic ([19, 20]), and hybrid ([21, 22]). For laminated composite beams, only some representative references are herein cited. For example, Khdeir and Reddy [23, 24] derived closed-form solutions of Reddy's theory for critical buckling loads and natural frequencies of cross-ply composite beams. Chandrashekhara and Bangera [25], Shi and Lam [26, 27], Murthy et al. [28] and Manur and Kant [29] investigated vibration behaviours of composite beams via finite element method (FEM). Karama et al. [30, 31] examined static, buckling and free vibration responses of composite beams based on trigonometric theory. Aydogdu [32–34] used polynomial, hyperbolic and exponential theories and the Ritz method to explore the behaviour of composite beams. Shao et al. [35] presented various HSBTs for the free vibration of composite beams. Vo and Thai [36–39] presented FEM solutions of both HSBT and quasi-3D theory for the structural analysis of composite beams. Mantari and Canales [40, 41] developed both Ritz and FEM solutions for composite beams by using the quasi-3D theories with a third-order, polynomial and hybrid polynomial-trigonometric theories. Matsunaga [42] considered free vibration responses of composite beams by means of quasi-3D theory and Navier procedure. By using Carrera Unified Formulation (CUF) [43], Carrera et al. [44–47] and Arruda et al. [48] analysed laminated composite beams. Vidal et al. [49] recently developed higher-order beam elements to model composite beams with generic cross-section.

This paper aims to propose a novel unified HSBT which can be recovered to existing HSBT by changing the shear functions. The Ritz solution method with novel hybrid shape functions is employed to develop approximate solutions for deflections, stresses, critical buckling loads and natural

frequencies of laminated composite beams under various boundary conditions and lay-ups. In order to validate the accuracy of the proposed theory, several numerical examples in static, vibration and buckling are considered. In addition, the effects of fibre orientation on the behaviour of laminated composite beams are also examined.

2. Theoretical formulation

2.1. A general framework of higher-order displacement field

For the simplicity purpose, it is supposed that the effects of the transverse normal strain is neglected and all formulations in this section are performed under the assumption of isotropic materials. The stress - strain relationships of the beam are therefore given by:

$$\epsilon_x = \frac{1}{E}\sigma_x \tag{1a}$$

$$\gamma_{xz} = \frac{1}{G}\sigma_{xz} \tag{1b}$$

in which E and G are Young's modulus and shear modulus, respectively. Moreover, the linear elastic relationships of strains and displacements are expressed by:

$$\epsilon_x = u_{,x} \tag{2a}$$

$$\gamma_{xz} = u_{,z} + w_{,x} \tag{2b}$$

in which u and w are respectively axial and transverse deflections. Substituting Eq. (2) into Eq. (1) leads to:

$$u_{,x} = \frac{1}{E}\sigma_x \tag{3a}$$

$$u_{,z} + w_{,x} = \frac{1}{G}\sigma_{xz} \tag{3b}$$

The transverse shear stress $\sigma_{xz}(x, z)$ can be expressed in terms of the transverse shear force $Q_x(x)$ as follows:

$$\sigma_{xz}(x, z) = g(z)Q_x(x) \tag{4}$$

where $g(z)$ is a higher-order shear function that satisfies the traction-free conditions at the bottom and top surfaces of the beam, i.e $g(z = \pm h/2) = 0$ with h being the beam thickness. Substituting Eq.

(4) into Eq. (3b) and taking into account the hypothesis of $w(x,z) = w_0(x)$, the axial displacement of the beam can be expressed by:

$$u(x,z) = u_0(x) - zw_{0,x} + f(z)\frac{Q_x(x)}{G} \tag{5}$$

where $f'(z) = g(z)$.

Therefore, a general formulation of the displacement field of the proposed theory is obtained as follows:

$$\begin{aligned} u(x,z) &= u_0(x) - zw_{0,x} + f(z)\frac{Q_x(x)}{G} && \text{(6a)} \\ w(x,z) &= w_0(x) && \text{(6b)} \end{aligned}$$

It can be noticed that when $f(z) = \frac{3}{2h}\left(z - \frac{4z^3}{3h^2}\right)$, Eq. (6) yields to the zeroth-order shear deformation theory developed by Shimpi [50] for plates. Moreover, if the shear force is expressed in the form:

$$Q_x = G\theta_0(x) \tag{7}$$

where θ_0 is the beam rotation, the displacement field in Eq. (6) becomes a common form of the HSBT, which has been widely used by many authors due to its simplicity:

$$\begin{aligned} u(x,z) &= u_0(x) - w_{0,x}z + f(z)\theta_0(x) && \text{(8a)} \\ w(x,z) &= w_0(x) && \text{(8b)} \end{aligned}$$

Furthermore, if the transverse shear force is written in terms of the rotation and the derivative of transverse deflection as follows ([7]):

$$Q_x = \frac{5Gh}{6}\left(\theta_0 + w_{0,x}\right) \tag{9}$$

Eq. (6) becomes a general formulation of the HSBT as follows:

$$\begin{aligned} u(x,z) &= u_0(x) + \left(\frac{5hf}{6} - z\right)w_{0,x} + \frac{5hf}{6}\theta_0(x) = u_0(x) + (\Phi - z)w_{0,x} + \Phi(z)\theta_0(x) && \text{(10a)} \\ w(x,z) &= w_0(x) && \text{(10b)} \end{aligned}$$

where $\Phi(z) = \frac{5h}{6}f(z)$.

The displacement field in Eq. (10) can be considered as an unified HSBT that many theories can be obtained. For example, the HSBT proposed by Reissner [7], Shi [26] and Reddy [9] can be recovered with $f(z) = \frac{3}{2h}\left(z - \frac{4z^3}{3h^2}\right)$ and $f(z) = \frac{6}{5h}\left(z - \frac{4z^3}{3h^2}\right)$, respectively.

2.2. Strain and stress fields

The non-zero strains associated to the displacements in Eq. (10) are therefore given by:

$$\epsilon_x(x,z) = u_{0,x} + (\Phi - z)w_{0,xx} + \Phi\theta_{0,x} \tag{11a}$$

$$\gamma_{xz}(x,z) = \Phi'(\theta_0 + w_{0,x}) \tag{11b}$$

The non-zero stresses at the k^{th}-layer of the beam associated to the strains in Eq. (11) are given by ([5]):

$$\sigma_x(x,z) = \bar{Q}_{11}\epsilon_x = \bar{Q}_{11}\Big[u_{0,x} + (\Phi - z)w_{0,xx} + \Phi\theta_{0,x}\Big] \tag{12a}$$

$$\sigma_{xz}(x,z) = \bar{Q}_{55}\gamma_{xz} = \bar{Q}_{55}\Phi'(\theta_0 + w_{0,x}) \tag{12b}$$

where

$$\bar{Q}_{11} = Q_{11} - \frac{Q_{13}^2}{Q_{33}}, \bar{Q}_{55} = Q_{55} \tag{13a}$$

$$Q_{11} = C'_{11} + \frac{C'^2_{16}C'_{22} - 2C'_{12}C'_{16}C'_{26} + C'^2_{12}C'_{66}}{C'^2_{26} - C'_{22}C'_{66}} \tag{13b}$$

$$Q_{13} = C'_{13} + \frac{C'_{16}C'_{22}C'_{36} + C'_{12}C'_{23}C'_{66} - C'_{16}C'_{23}C'_{26} - C'_{12}C'_{26}C'_{36}}{C'^2_{26} - C'_{22}C'_{66}} \tag{13c}$$

$$Q_{33} = C'_{33} + \frac{C'^2_{36}C'_{22} - 2C'_{23}C'_{26}C'_{36} + C'^2_{23}C'_{66}}{C'^2_{26} - C'_{22}C'_{66}} \tag{13d}$$

$$Q_{55} = C'_{55} - \frac{C'^2_{45}}{C'_{44}} \tag{13e}$$

where C'_{ij} are the elastic stiffness coefficients at the k^{th}-layer of the beam (see [51] for more details).

2.3. Governing equations of motion

The strain energy of the proposed beam model can be written as:

$$\begin{aligned}\mathcal{U} &= \frac{1}{2}\int_V (\sigma_x\epsilon_x + \sigma_{xz}\gamma_{xz})dV \\ &= \frac{1}{2}\int_0^L \Big[Au_{0,x}^2 + 2Bu_{0,x}w_{0,xx} + Dw_{0,xx}^2 + 2B^s u_{0,x}\theta_{0,x} + 2D^s w_{0,xx}\theta_{0,x} + H^s\theta_{0,x}^2 \\ &+ A^s(\theta_0^2 + w_{0,x}^2 + 2\theta_0 w_{0,x})\Big]dx\end{aligned} \tag{14}$$

where (A, A^s, B, B^s, D, D^s and H^s) are the stiffness coefficients defined as:

$$\Big\{A, B, D, B^s, D^s, H^s\Big\} = \int_{-h/2}^{h/2} \Big\{1, \Phi - z, (\Phi - z)^2, \Phi, (\Phi - z)\Phi, \Phi^2\Big\}\bar{Q}_{11}bdz \tag{15}$$

$$A^s = \int_{-h/2}^{h/2} \Phi'^2\bar{Q}_{55}bdz \tag{16}$$

The external work done by the transverse load q and axial compression N_0 is obtained as follows:

$$\mathcal{V} = -\int_0^L q w_0 dx - \frac{1}{2}\int_0^L N_0 w_{0,x}^2 dx \tag{17}$$

The kinetic energy of the proposed beam model is calculated by:

$$\begin{aligned}\mathcal{K} &= \frac{1}{2}\int_V \rho(z)(\dot{u}^2 + \dot{w}^2)dV \\ &= \frac{1}{2}\int_0^L \Big[I_0\dot{u}_0^2 + 2I_1\dot{u}_0\dot{w}_{0,x} + I_2\dot{w}_{0,x}^2 + 2J_1\dot{\theta}_0\dot{u}_0 + 2J_2\dot{\theta}_0\dot{w}_{0,x} + K_2\dot{\theta}_0^2 + I_0\dot{w}_0^2\Big]dx\end{aligned} \tag{18}$$

in which dot-superscript indicates time derivative t; ρ is the mass density; and the moment of inertia terms $I_0, I_1, I_2, J_1, J_2, K_2$ are defined as:

$$\Big\{I_0, I_1, I_2, J_1, J_2, K_2\Big\} = \int_{-h/2}^{h/2}\Big\{1, \Phi - z, (\Phi - z)^2, \Phi, (\Phi - z)\Phi, \Phi^2\Big\}\rho b dz \tag{19}$$

Finally, the total energy of the beam is obtained as:

$$\begin{aligned}\Pi &= \mathcal{U} + \mathcal{V} - \mathcal{K} \\ &= \frac{1}{2}\int_0^L \Big[Au_{0,x}^2 + 2Bu_{0,x}w_{0,xx} + Dw_{0,xx}^2 + 2B^s u_{0,x}\theta_{0,x} + 2D^s w_{0,xx}\theta_{0,x} + H^s\theta_{0,x}^2 \\ &+ A^s(\theta_0^2 + w_{0,x}^2 + 2\theta_0 w_{0,x})\Big]dx - \frac{1}{2}\int_0^L N_0 w_{0,x}^2 dx - \int_0^L q w_0 dx \\ &- \frac{1}{2}\int_0^L \Big[I_0\dot{u}_0^2 + 2I_1\dot{u}_0\dot{w}_{0,x} + I_2\dot{w}_{0,x}^2 + 2J_1\dot{\theta}_0\dot{u}_0 + 2J_2\dot{\theta}_0\dot{w}_{0,x} + K_2\dot{\theta}_0^2 + I_0\dot{w}_0^2\Big]dx\end{aligned} \tag{20}$$

Based on the Ritz method [51], the displacement variables in Eq. (20) can be approximated as:

$$u_0(x,t) = \sum_{j=1}^m \psi_x(x)u_j e^{i\omega t} \tag{21a}$$

$$w_0(x,t) = \sum_{j=1}^m \varphi_j(x)w_j e^{i\omega t} \tag{21b}$$

$$\theta_0(x,t) = \sum_{j=1}^m \psi_x(x)\theta_j e^{i\omega t} \tag{21c}$$

where ω is the frequency, $i^2 = -1$; (u_j, w_j, θ_j) are unknown variables;$\psi_j(x)$ and $\varphi_j(x)$ are the shape functions which should be chosen to satisfy the boundary conditions [51]. If they do not meet these conditions, a penalty function method can be applied to recover the boundary conditions [52]. Practically however, this approach leads to an increase in the size of the stiffness and mass matrices and thus causing computational costs. Moreover, it is known that the equations of motion of the beams are expressed under the fourth-order differential ones, hence the primary solutions are given in terms of exponential functions. It is numerically observed that the approximation of field variables based on the

elastic homogeneous solution will lead to an accuracy and fast convergence of the solution. Therefore, the present research proposes novel hybrid shape functions given in Table 1. These functions are composed of the exponential functions and admissible trigonometric ones that satisfy automatically various boundary conditions of the beam given in Table 2 in which S-S, C-F and C-C are represented for simply supported, clamped-free and clamped-clamped, respectively.

The governing equations of motion can be obtained in the form of Lagrange's equations by substituting Eq. (21) into Eq. (20)

$$\frac{\partial \Pi}{\partial d_j} - \frac{d}{dt}\frac{\partial \Pi}{\partial \dot{d}_j} = 0 \tag{22}$$

where d_j represents for (u_j, w_j, θ_j).

Eq. (22) can be written in the matrix forms as:

$$\left(\begin{bmatrix} \mathbf{K}^{11} & \mathbf{K}^{12} & \mathbf{K}^{13} \\ {}^{T}\mathbf{K}^{12} & \mathbf{K}^{22} & \mathbf{K}^{23} \\ {}^{T}\mathbf{K}^{13} & {}^{T}\mathbf{K}^{23} & \mathbf{K}^{33} \end{bmatrix} - \omega^2 \begin{bmatrix} \mathbf{M}^{11} & \mathbf{M}^{12} & \mathbf{M}^{13} \\ {}^{T}\mathbf{M}^{12} & \mathbf{M}^{22} & \mathbf{M}^{23} \\ {}^{T}\mathbf{M}^{13} & {}^{T}\mathbf{M}^{23} & \mathbf{M}^{33} \end{bmatrix} \right) \begin{Bmatrix} \mathbf{u} \\ \mathbf{w} \\ \boldsymbol{\theta} \end{Bmatrix} = \begin{Bmatrix} \mathbf{0} \\ \mathbf{F} \\ \mathbf{0} \end{Bmatrix} \tag{23}$$

or under the compact form:

$$(\mathbf{K} - \omega^2 \mathbf{M})\mathbf{d} = \mathbf{P} \tag{24}$$

where the components of the stiffness matrix $\mathbf{K}$, mass matrix $\mathbf{M}$ and force vector $\mathbf{P}$ are given by:

$$\begin{aligned}
K_{ij}^{11} &= A\int_0^L \psi_{i,x}\psi_{j,x}\,dx, K_{ij}^{12} = B\int_0^L \psi_{i,x}\varphi_{j,xx}\,dx, K_{ij}^{13} = B^s\int_0^L \psi_{i,x}\psi_{j,x}\,dx \\
K_{ij}^{22} &= \int_0^L (D\varphi_{i,xx}\varphi_{j,xx} + A^s\varphi_{i,x}\varphi_{j,x} - N^0\varphi_{i,x}\varphi_{j,x})\,dx \\
K_{ij}^{23} &= \int_0^L (D^s\varphi_{i,xx}\psi_{j,x} + A^s\varphi_{i,x}\psi_j)\,dx, K_{ij}^{33} = \int_0^L (H^s\psi_{i,x}\psi_{j,x} + A^s\psi_i\psi_j)\,dx \\
M_{ij}^{11} &= I_0\int_0^L \psi_i\psi_j\,dx, M_{ij}^{12} = I_1\int_0^L \psi_i\varphi_{j,x}\,dx, M_{ij}^{13} = J_1\int_0^L \psi_i\psi_j\,dx, \\
M_{ij}^{22} &= \int_0^L (I_0\varphi_i\varphi_j + I_2\varphi_{i,x}\varphi_{j,x})\,dx, M_{ij}^{23} = J_2\int_0^L \varphi_{i,x}\psi_j\,dx, M_{ij}^{33} = K_2\int_0^L \psi_i\psi_j\,dx \\
F_i &= \int_0^L q\varphi_i dx
\end{aligned} \tag{25}$$

It is noted from Eq. (24) that the bending responses can be derived by solving the equation $\mathbf{Kd} = \mathbf{P}$, the buckling responses by solving the equation $|\mathbf{K}| = 0$, and vibration responses based on the equation $|\mathbf{K} - \omega^2\mathbf{M}|$=0.

3. Numerical examples

To demonstrate the accuracy of the proposed beam model, two shear functions $f(z)$ involved in Eq. (10) are considered: $f(z) = \frac{3}{2h}\left(z - \frac{4z^3}{3h^2}\right)$ [7] (HSBT1) and $f(z) = \frac{h}{\pi}\sin\frac{\pi z}{h}$ [13] (HSBT2). Several cases in static, vibration and buckling of laminated composite beams are carried out to validate the proposed theory. The following materials are used:

- Material I [32]: $E_2 = E_3$, $G_{12} = G_{13} = 0.6E_2, G_{23} = 0.5E_2, \nu_{12} = \nu_{13} = \nu_{23} = 0.25$
- Material II [32]: $E_2 = E_3$, $G_{12} = G_{13} = 0.5E_2, G_{23} = 0.2E_2, \nu_{12} = \nu_{13} = \nu_{23} = 0.25$

For convenience, the following normalized terms are used:

$$\bar{w} = \frac{100 w_0 E_2 b h^3}{qL^4}, \bar{\sigma}_{xx} = \frac{bh^2}{qL^2}\sigma_{xx}\left(\frac{L}{2}, \frac{h}{2}\right), \bar{\sigma}_{xz} = \frac{bh}{qL}\sigma_{xz}(0,0) \tag{26a}$$

$$\bar{\omega} = \frac{\omega L^2}{h}\sqrt{\frac{\rho}{E_2}} \tag{26b}$$

$$\bar{N}_{cr} = N_{cr}\frac{L^2}{E_2 b h^3} \tag{26c}$$

The Ritz method has been widely used for bending, vibration and buckling analysis of the structures. The static responses are related to the equilibrium problem while the buckling and vibration behaviours correspond to the eigenvalue ones. It is from many previous works that this method yields upper bound to the exact values for the natural frequencies and buckling loads, and lower bound for the displacements in average sense (see Refs. [53–55] for more details). In order to verify the convergence of the present solutions, a $(0^o/90^o/0^o)$ composite beam for different boundary conditions with Material I, E_1/E_2=40 and L/h=5 has been considered and its results are shown in Table 3. It can be seen that the present solutions converge when the number of series m=12. Therefore, this value will be used herein for the following numerical examples. It is also observed from Table 3 that the solutions of C-F and C-C beams converge slower than that of S-S beam due to essential boundary conditions.

3.1. Bending analysis

Table 4 shows nondimensional mid-span displacements of $(0^o/90^o/0^o)$ and $(0^o/90^o)$ composite beams with Material II and E_1/E_2=25. The results are reported for S-S, C-C and C-F beams with three different span-to-thickness ratios L/h=5, 10 and 50. The present solutions are also compared with those obtained from the HSBTs of Nguyen et al. [4], Murthy et al. [28], Khdeir and Reddy [56], and the quasi-3D theories of Nguyen et al. [5], Zenkour [57]. It can be observed that that all present solutions agree well with existing solutions. In addition, the transverse displacements of HSBT1 are

closer to those of quasi-3D theory [5, 57] than those of the HSBT2, however the HSBTs converge each other when the effect of shear deformation is small ($L/h = 50$). The comparison of normal stress and shear stress are also introduced in Table 5 for S-S beams. Again, excellent agreements between these HSBTs are found.

To investigate the influence of fibre angle change on the static responses, Table 6 presents the nondimensional transverse mid-span displacements of $(0^o/\theta^o/0^o)$ and $(0^o/\theta^o)$ laminated composite beams with $L/h = 10$ and Material II (E_1/E_2=25). The results are displayed with various fibre angles and for different boundary conditions, and then compared with those from the quasi-3D theory of Nguyen et al. [5]. As expected, the present results comply with those from the previous work. The variation of the transverse displacements with fibre angles for S-S beams is illustrated in Fig. 2. It can be seen that the deflections of $(0^o/\theta^o)$ beams increase by the increase of the fibre orientation and change rapidly from θ=5^o to θ=70^o. Whereas, the displacements obtained from symmetric beams $(0^o/\theta^o/0^o)$ are quite small in comparison with those of asymmetric ones $(0^o/\theta^o)$, which can be explained by the differences between flexural stiffness of two lay-ups.

3.2. Buckling and free vibration analyses

The comparisons of the normalized fundamental frequencies are presented in Tables 7 and 8, whilst the comparisons of the normalized critical buckling loads are presented in Tables 9 and 10. The comparison is made for different beam configurations, i.e., $(0^o/90^o/0^o)$, $(0^o/90^o)$, $(0^o/\theta^o/0^o)$ and $(0^o/\theta^o)$ under various span-to-thickness ratios, fibre orientations and boundary conditions. It is noted that although the bifurcation buckling phenomena does not occur for laminated composite beams with unsymmetric layers, in order to verify the accuracy of the present beam theory in comparison with the earlier researches, the critical buckling loads of laminated composite beams with layers $(0^o/90^o)$ and $(0^o/\theta^o)$ are still considered. The validation of these results are compared with those derived from the HSBTs ([4, 24, 28]) and quasi-3D theories ([5, 40, 42]). It can be seen that the consistencies of the solutions are again found.

The influence of fibre orientation on the normalized fundamental natural frequencies and critical buckling loads of $(0^o/\theta^o/0^o)$ and $(0^o/\theta^o)$ laminated composite beams are displayed in Figs. 3 and 4, respectively, for S-S beams. It can be seen that the increase of fibre angle leads an decrease in the buckling loads and fundamental frequencies. The significant deviations on the results of asymmetric beams are observed from θ=5^o to θ=70^o, which is the same response with the transverse displacement.

4. Conclusions

A novel unified beam theory has been proposed for the bending, buckling and free vibration analysis of composite beams. Based on the fundamental equations of elasticity theory, the displacement field of the proposed model was derived in a unified form which can be recovered to that of existing HSBTs available in the literature. The Ritz method with a new shape function under hybrid form has been employed to solve the governing equations of the proposed beam model for stresses, deflections, buckling loads and natural frequencies. A comprehensive verification study has been conducted, and the numerical results demonstrated that the proposed beam model can well predict the bending, free vibration and buckling responses of composite beams under different boundary conditions and arbitrary lay-ups. In addition, the comprehensive result presented in this paper can also be served as a reference solution for the development of composite beam models in the future.

Acknowledgements

This research is funded by Vietnam National Foundation for Science and Technology Development (NAFOSTED) under Grant No. 107.02-2018.312.

References

[1] Y. M. Ghugal, R. P. Shimpi, A review of refined shear deformation theories for isotropic and anisotropic laminated beams, Journal of Reinforced Plastics and Composites 20 (3) (2001) 255–272.

[2] R. Aguiar, F. Moleiro, C. M. Soares, Assessment of mixed and displacement-based models for static analysis of composite beams of different cross-sections, Composite Structures 94 (2) (2012) 601 – 616.

[3] W. Zhen, C. Wanji, An assessment of several displacement-based theories for the vibration and stability analysis of laminated composite and sandwich beams, Composite Structures 84 (4) (2008) 337–349.

[4] T.-K. Nguyen, N.-D. Nguyen, T. P. Vo, H.-T. Thai, Trigonometric-series solution for analysis of laminated composite beams, Composite Structures 160 (2017) 142–151.

[5] N.-D. Nguyen, T.-K. Nguyen, T. P. Vo, H.-T. Thai, Ritz-based analytical solutions for bending, buckling and vibration behavior of laminated composite beams, International Journal of Structural Stability and Dynamics 18 (11) (2018) 1850130.

[6] S. Ambartsumian, On the theory of bending of anisotropic plates and shallow shells, Journal of Applied Mathematics and Mechanics 24 (2) (1960) 500–514.

[7] E. Reissner, On transverse bending of plates, including the effect of transverse shear deformation, International Journal of Solids and Structures 11 (5) (1975) 569–573.

[8] M. Levinson, An accurate, simple theory of the statics and dynamics of elastic plates, Mechanics Research Communications 7 (6) (1980) 343–350.

[9] J. N. Reddy, A Simple Higher-Order Theory for Laminated Composite Plates, Journal of Applied Mechanics 51 (4) (1984) 745–752.

[10] T. N. Nguyen, C. H. Thai, H. Nguyen-Xuan, On the general framework of high order shear deformation theories for laminated composite plate structures: A novel unified approach, International Journal of Mechanical Sciences 110 (2016) 242–255.

[11] M. Murthy, An improved transverse shear deformation theory for laminated anisotropic plates, National Aeronautics and Space Administration, Washington DC, 1981.

[12] M. STEIN, Nonlinear theory for plates and shells including the effects of transverse shearing, AIAA Journal 24 (9) (1986) 1537–1544.

[13] M. Touratier, An efficient standard plate theory, International Journal of Engineering Science 29 (8) (1991) 901–916.

[14] H. Arya, R. Shimpi, N. Naik, A zigzag model for laminated composite beams, Composite Structures 56 (1) (2002) 21–24.

[15] C. H. Thai, A. Ferreira, S. Bordas, T. Rabczuk, H. Nguyen-Xuan, Isogeometric analysis of laminated composite and sandwich plates using a new inverse trigonometric shear deformation theory, European Journal of Mechanics - A/Solids 43 (2014) 89–108.

[16] J. Mantari, A. Oktem, C. G. Soares, A new trigonometric shear deformation theory for isotropic, laminated composite and sandwich plates, International Journal of Solids and Structures 49 (1) (2012) 43–53.

[17] V.-H. Nguyen, T.-K. Nguyen, H.-T. Thai, T. P. Vo, A new inverse trigonometric shear deformation theory for isotropic and functionally graded sandwich plates, Composites Part B: Engineering 66 (2014) 233–246.

[18] M. Aydogdu, A new shear deformation theory for laminated composite plates, Composite Structures 89 (1) (2009) 94–101.

[19] K. P. Soldatos, A transverse shear deformation theory for homogeneous monoclinic plates, Acta Mechanica 94 (3) (1992) 195–220.

[20] S. S. Akavci, A. H. Tanrikulu, Buckling and free vibration analyses of laminated composite plates by using two new hyperbolic shear-deformation theories, Mechanics of Composite Materials 44 (2) (2008) 145–154.

[21] J. Mantari, A. Oktem, C. G. Soares, A new higher order shear deformation theory for sandwich and composite laminated plates, Composites Part B: Engineering 43 (3) (2012) 1489–1499.

[22] C. H. Thai, S. Kulasegaram, L. V. Tran, H. Nguyen-Xuan, Generalized shear deformation theory for functionally graded isotropic and sandwich plates based on isogeometric approach, Computers & Structures 141 (2014) 94–112.

[23] A. Khdeir, J. Reddy, Free vibration of cross-ply laminated beams with arbitrary boundary conditions, International Journal of Engineering Science 32 (12) (1994) 1971–1980.

[24] A. Khdeir, J. Redd, Buckling of cross-ply laminated beams with arbitrary boundary conditions, Composite Structures 37 (1) (1997) 1–3.

[25] K. Chandrashekhara, K. Bangera, Free vibration of composite beams using a refined shear flexible beam element, Computers & Structures 43 (4) (1992) 719 – 727.

[26] G. Shi, K. Lam, T. Tay, On efficient finite element modeling of composite beams and plates using higher-order theories and an accurate composite beam element, Composite Structures 41 (2) (1998) 159–165.

[27] G. Shi, K. Lam, Finite element vibration analysis of composite beams based on higher-order beam theory, Journal of Sound and Vibration 219 (4) (1999) 707 – 721.

[28] M. Murthy, D. R. Mahapatra, K. Badarinarayana, S. Gopalakrishnan, A refined higher order finite element for asymmetric composite beams, Composite Structures 67 (1) (2005) 27 – 35.

[29] S. Marur, T. Kant, Free vibration analysis of fiber reinforced composite beams using higher order theories and finite element modelling, Journal of Sound and Vibration 194 (3) (1996) 337 – 351.

[30] M. Karama, B. A. Harb, S. Mistou, S. Caperaa, Bending, buckling and free vibration of laminated composite with a transverse shear stress continuity model, Composites Part B: Engineering 29 (3) (1998) 223 – 234.

[31] M. Karama, K. Afaq, S. Mistou, Mechanical behaviour of laminated composite beam by the new multi-layered laminated composite structures model with transverse shear stress continuity, International Journal of Solids and Structures 40 (6) (2003) 1525 – 1546.

[32] M. Aydogdu, Vibration analysis of cross-ply laminated beams with general boundary conditions by ritz method, International Journal of Mechanical Sciences 47 (11) (2005) 1740 – 1755.

[33] M. Aydogdu, Buckling analysis of cross-ply laminated beams with general boundary conditions by ritz method, Composites Science and Technology 66 (10) (2006) 1248 – 1255.

[34] M. Aydogdu, Free vibration analysis of angle-ply laminated beams with general boundary conditions, Journal of Reinforced Plastics and Composites 25 (15) (2006) 1571–1583.

[35] D. Shao, S. Hu, Q. Wang, F. Pang, Free vibration of refined higher-order shear deformation composite laminated beams with general boundary conditions, Composites Part B: Engineering 108 (2017) 75 – 90.

[36] T. P. Vo, H.-T. Thai, Static behavior of composite beams using various refined shear deformation theories, Composite Structures 94 (8) (2012) 2513 – 2522.

[37] T. P. Vo, H.-T. Thai, Vibration and buckling of composite beams using refined shear deformation theory, International Journal of Mechanical Sciences 62 (1) (2012) 67 – 76.

[38] T. P. Vo, H.-T. Thai, T.-K. Nguyen, D. Lanc, A. Karamanli, Flexural analysis of laminated composite and sandwich beams using a four-unknown shear and normal deformation theory, Composite Structures 176 (2017) 388 – 397.

[39] T. P. Vo, H.-T. Thai, M. Aydogdu, Free vibration of axially loaded composite beams using a four-unknown shear and normal deformation theory, Composite Structures 178 (2017) 406 – 414.

[40] J. Mantari, F. Canales, Free vibration and buckling of laminated beams via hybrid ritz solution for various penalized boundary conditions, Composite Structures 152 (2016) 306–315.

[41] J. Mantari, F. Canales, Finite element formulation of laminated beams with capability to model the thickness expansion, Composites Part B: Engineering 101 (2016) 107–115.

[42] H. Matsunaga, Vibration and buckling of multilayered composite beams according to higher order deformation theories, Journal of Sound and Vibration 246 (1) (2001) 47–62.

[43] M. P. Erasmo Carrera, Gaetano Giunta, Beam Structures: Classical and Advanced Theories, Wiley, 2011.

[44] E. Carrera, M. Filippi, E. Zappino, Laminated beam analysis by polynomial, trigonometric, exponential and zig-zag theories, European Journal of Mechanics - A/Solids 41 (2013) 58 – 69.

[45] G. Giunta, F. Biscani, S. Belouettar, A. Ferreira, E. Carrera, Free vibration analysis of composite beams via refined theories, Composites Part B: Engineering 44 (1) (2013) 540–552.

[46] M. Filippi, E. Carrera, Bending and vibrations analyses of laminated beams by using a zig-zag-layer-wise theory, Composites Part B: Engineering 98 (2016) 269–280.

[47] A. Pagani, A. de Miguel, M. Petrolo, E. Carrera, Analysis of laminated beams via unified formulation and legendre polynomial expansions, Composite Structures 156 (2016) 78 – 92, 70th Anniversary of Professor J. N. Reddy.

[48] M. Arruda, L. Castro, A. Ferreira, M. Garrido, J. Gonilha, J. Correia, Analysis of composite layered beams using carrera unified formulation with legendre approximation, Composites Part B: Engineering 137 (2018) 39–50.

[49] P. Vidal, G. Giunta, L. Gallimard, O. Polit, Modeling of composite and sandwich beams with a generic cross-section using a variable separation method, Composites Part B: Engineering 165 (2019) 648–661.

[50] R. P. Shimpi, Zeroth-order shear deformation theory for plates, AIAA Journal 37 (4) (1999) 524–526.

[51] J. N. Reddy, Mechanics of Laminated Composites Plates: Theory and Analysis, CRC Press, Boca Raton, 1997.

[52] T.-K. Nguyen, T. T.-P. Nguyen, T. P. Vo, H.-T. Thai, Vibration and buckling analysis of functionally graded sandwich beams by a new higher-order shear deformation theory, Composites Part B: Engineering 76 (2015) 273 – 285.

[53] R. Courant, Variational methods for the solution of problems of equilibrium and vibrations, Bulletin of the American Mathematical Society 49 (1943) 1–23.

[54] R. Courant, D. Hilbert, Methods of Mathematical Physics, Wiley, 1989.

[55] A. W. Leissa, S. M. Shihada, Convergence of the ritz method, Applied Mechanics Reviews 48 (115) (1995) 590–595.

[56] A. Khdeir, J. Reddy, An exact solution for the bending of thin and thick cross-ply laminated beams, Composite Structures 37 (2) (1997) 195–203.

[57] A. M. Zenkour, Transverse shear and normal deformation theory for bending analysis of laminated and sandwich elastic beams, Mechanics of Composite Materials and Structures 6 (3) (1999) 267–283.

CAPTIONS OF TABLES

Table 1: Hybrid shape functions of the Ritz method.

Table 2: Boundary conditions of the proposed beam model.

Table 3: Convergence studies for $(0^o/90^o/0^o)$ composite beams ($L/h = 5$, HSBT1, Material I, $E_1/E_2 = 40$).

Table 4: Normalized deflections of $(0^o/90^o/0^o)$ and $(0^o/90^o)$ beams under uniform loads (Material II, E_1/E_2=25).

Table 5: Normalized stresses of $(0^o/90^o/0^o)$ and $(0^o/90^o)$ S-S beams under uniform loads (Material II, E_1/E_2=25).

Table 6: Normalized deflections of $[0^o/\theta^o/0^o]$ and $[0^o/\theta^o]$ beams under uniform loads (L/h=10, Materials II, E_1/E_2=25).

Table 7: Normalized fundamental frequencies of $(0^o/90^o/0^o)$ and $(0^o/90^o)$ composite beams (Material I, E_1/E_2=40).

Table 8: Normalized fundamental frequencies of $[0^o/\theta^o/0^o]$ and $[0^o/\theta^o]$ composite beams (L/h=10, Materials I, E_1/E_2=40).

Table 9: Normalized buckling loads of $(0^o/90^o/0^o)$ and $(0^o/90^o)$ composite beams (Material I, E_1/E_2=40).

Table 10: Normalized buckling loads of $[0^o/\theta^o/0^o]$ and $[0^o/\theta^o]$ composite beams (L/h=10, Materials I, E_1/E_2=40).

CAPTIONS OF FIGURES

Figure 1: Geometric dimensions of a typical laminated composite beam.

Figure 2: Influences of fibre orientation on normalized deflections of $[0^o/\theta^o/0^o]$ and $[0^o/\theta^o]$ composite beams under uniform loads (L/h=10, Material II, E_1/E_2=25).

Figure 3: Influences of fibre orientation on normalized fundamental frequencies of $[0^o/\theta^o/0^o]$ and $[0^o/\theta^o]$ beams (L/h=10, Material I, E_1/E_2=40).

Figure 4: Influences of fibre orientation on normalized critical buckling loads of $[0^o/\theta^o/0^o]$ and $[0^o/\theta^o]$ beams (L/h=10, Material I, E_1/E_2=40).

Table 1: Hybrid shape functions of the Ritz method.

Boundary conditions	$\varphi_j(x)$	$\psi_j(x)$
S-S	$\sin\frac{\pi x}{L}\, e^{-\frac{jx}{L}}$	$\cos\frac{j\pi x}{L}\ \ e^{-\frac{jx}{L}}$
C-F	$(1-\cos\frac{\pi x}{2L})\ \ e^{-\frac{jx}{L}}$	$\sin\frac{\pi x}{2L}\ \ e^{-\frac{jx}{L}}$
C-C	$\sin^2\frac{\pi x}{L}\ \ e^{-\frac{jx}{L}}$	$\sin\frac{\pi x}{L}\ \ e^{-\frac{jx}{L}}$

Table 2: Boundary conditions of the proposed beam model.

Beam	$x = 0$	$x = L$
S-S	$w_0 = 0$	$w_0 = 0$
C-C	$u_0 = 0$, $w_0 = 0$, θ_0=0, $w_{0,x}$=0	$u_0 = 0$, $w_0 = 0$, θ_0=0, $w_{0,x}$=0
C-F	$u_0 = 0$, $w_0 = 0$, θ_0=0, $w_{0,x}$=0	

Table 3: Convergence studies for $(0^o/90^o/0^o)$ composite beams ($L/h = 5$, HSBT1, Material I, $E_1/E_2 = 40$).

Beam	Number of terms in series (m)						
	2	4	6	8	10	12	14
Transverse displacement							
S-S	1.4689	1.4664	1.4679	1.4677	1.4675	1.4682	1.4680
C-F	3.8906	4.1365	4.1686	4.1678	4.1675	4.1662	4.1661
C-C	0.8232	0.8940	0.9263	0.9321	0.9327	0.9316	0.9321
Fundamental frequency							
S-S	9.3215	9.2080	9.2062	9.2062	9.2062	9.2062	9.2062
C-F	4.3362	4.2373	4.2309	4.2304	4.2298	4.2295	4.2297
C-C	12.6368	11.7766	11.6348	11.6094	11.6052	11.6047	11.6043
Critical buckling load							
S-S	8.7232	8.6116	8.6093	8.6092	8.6092	8.6092	8.6092
C-F	4.9610	4.7075	4.7035	4.7034	4.7029	4.7028	4.7025
C-C	11.8736	11.6514	11.6484	11.6482	11.6478	11.6475	11.6471

Table 4: Normalized deflections of ($0^o/90^o/0^o$) and ($0^o/90^o$) beams under uniform loads (Material II, E_1/E_2=25).

Beam	Theory	$0^o/90^o/0^o$			$0^o/90^o$		
		5	10	50	5	10	50
S-S	HSBT1	2.413	1.098	0.666	4.785	3.696	3.344
	HSBT2	2.442	1.107	0.666	4.747	3.688	3.344
	HSBT [4]	2.412	1.096	0.665	4.777	3.688	3.336
	HSBT [28]	2.398	1.090	0.661	4.750	3.668	3.318
	HSBT [56]	2.412	1.096	0.666	4.777	3.688	3.336
	Quasi-3D [57]	2.405	1.097	0.666	4.828	3.763	3.415
	Quasi-3D [5]	2.405	1.097	0.666	4.764	3.694	3.345
C-F	HSBT1	6.825	3.459	2.257	15.301	12.370	11.366
	HSBT2	6.840	3.476	2.257	15.173	12.340	11.364
	HSBT [4]	6.813	3.447	2.250	15.260	12.330	11.335
	HSBT [28]	6.836	3.466	2.262	15.334	12.398	11.392
	HSBT [56]	6.824	3.455	2.251	15.279	12.343	11.337
	Quasi-3D [5]	6.844	3.451	2.256	15.260	12.339	11.343
C-C	HSBT1	1.539	0.531	0.147	1.920	1.004	0.679
	HSBT2	1.483	0.515	0.146	1.822	0.976	0.679
	HSBT [4]	1.536	0.531	0.147	1.920	1.004	0.679
	HSBT [56]	1.537	0.532	0.147	1.922	1.005	0.679
	Quasi-3D [5]	1.543	0.532	0.147	1.916	1.005	0.679

Table 5: Normalized stresses of ($0^o/90^o/0^o$) and ($0^o/90^o$) S-S beams under uniform loads (Material II, E_1/E_2=25).

Stress	Theory	$0^o/90^o/0^o$			$0^o/90^o$		
		5	10	50	5	10	50
$\bar{\sigma}_x$	HSBT1	1.0656	0.8493	0.7791	0.2360	0.2338	0.2332
	HSBT2	1.0787	0.8515	0.7800	0.2356	0.2341	0.2334
	HSBT [4]	1.0696	0.8516	-	0.2362	0.2343	-
	HSBT [57]	1.0669	0.8500	0.7805	0.2362	0.2343	0.2336
	HSBT [36]	1.0670	0.8503	-	0.2361	0.2342	-
	Quasi-3D [57]	1.0732	0.8506	0.7806	0.2276	0.2246	0.2236
	Quasi-3D [40]	-	0.8501	-	-	0.2227	-
	Quasi-3D [5]	1.0732	0.8504	0.7806	0.2380	0.2346	0.2336
$\bar{\sigma}_{xz}$	HSBT1	0.4047	0.4273	0.4522	0.9160	0.9560	0.9760
	HSBT2	0.4226	0.4496	0.4585	0.9281	0.9569	0.9794
	HSBT [4]	0.4050	0.4289	-	0.9174	0.9483	-
	HSBT [57]	0.4057	0.4311	0.4514	0.9211	0.9572	0.9860
	HSBT [36]	0.4057	0.4311	-	0.9187	0.9484	-
	Quasi-3D [57]	0.4013	0.4289	0.4509	0.9038	0.9469	0.9814
	Quasi-3D [40]	-	-	-	-	0.9503	-
	Quasi-3D [5]	0.4013	0.4286	0.4521	0.9052	0.9476	0.9869

Table 6: Normalized deflections of $[0^o/\theta^o/0^o]$ and $[0^o/\theta^o]$ beams under uniform loads (L/h=10, Materials II, E_1/E_2=25).

Lay-up	Beam	Theory	Fibre angle						
			0^o	15^o	30^o	45^o	60^o	75^o	90^o
$0^o/\theta^o/0^o$	S-S	HSBT1	0.9235	0.9542	0.9959	1.0383	1.0713	1.0912	1.0978
		HSBT2	0.9224	0.9534	0.9971	1.0423	1.0780	1.0997	1.1069
		HSBT [38]	0.9222	0.9529	0.9946	1.0370	1.0700	1.0900	1.0965
		Quasi-3D [5]	0.9222	0.9529	0.9946	1.0370	1.0700	1.0900	1.0965
	C-F	HSBT1	2.9653	3.0642	3.1815	3.2976	3.3873	3.4412	3.4589
		HSBT2	2.9576	3.0573	3.1795	3.3026	3.3987	3.4570	3.4763
		HSBT [38]	2.9663	3.0653	3.1828	3.2992	3.3889	3.4428	3.4605
		Quasi-3D [5]	2.9647	3.0636	3.1810	3.2973	3.3871	3.4412	3.4511
	C-C	HSBT1	0.3946	0.4107	0.4446	0.4806	0.5086	0.5254	0.5310
		HSBT2	0.3776	0.3931	0.4267	0.4630	0.4916	0.5089	0.5147
		HSBT [38]	0.3968	0.4130	0.4469	0.4828	0.5108	0.5277	0.5332
		Quasi-3D [5]	0.3958	0.4120	0.4459	0.4818	0.5098	0.5266	0.5323
$0^o/\theta^o$	S-S	HSBT1	0.9235	1.6888	2.7480	3.3513	3.6092	3.6863	3.6964
		HSBT2	0.9224	1.6866	2.7430	3.3443	3.6011	3.6777	3.6877
		HSBT [38]	0.9222	1.6861	2.7403	3.3370	3.5871	3.6562	3.6626
		Quasi-3D [5]	0.9222	1.6876	2.7463	3.3492	3.6070	3.6841	3.6942
	C-F	HSBT1	2.9653	5.5753	9.1744	11.2159	12.0830	12.3381	12.3702
		HSBT2	2.9576	5.5651	9.1557	11.1913	12.0551	12.3087	12.3404
		HSBT [38]	2.9663	5.5712	9.1499	11.1650	12.0020	12.2260	12.2440
		Quasi-3D [5]	2.9647	5.5734	9.1667	11.2026	12.0630	12.3104	12.3387
	C-C	HSBT1	0.3946	0.5562	0.7776	0.9118	0.9757	0.9994	1.0043
		HSBT2	0.3776	0.5375	0.7559	0.8873	0.9493	0.9719	0.9765
		HSBT [38]	0.3968	0.5584	0.7783	0.9107	0.9726	0.9943	0.9983
		Quasi-3D [5]	0.3958	0.5581	0.7797	0.9137	0.9771	1.0003	1.0050

Table 7: Normalized fundamental frequencies of ($0^o/90^o/0^o$) and ($0^o/90^o$) composite beams (Material I, E_1/E_2=40).

BC	Theory	$0^o/90^o/0^o$			$0^o/90^o$		
		5	10	50	5	10	50
S-S	HSBT1	9.206	13.607	17.449	6.125	6.940	7.297
	HSBT2	9.223	13.608	17.449	6.149	6.948	7.297
	HSBT [4]	9.208	13.614	17.462	6.128	6.945	7.302
	HSBT [28]	9.207	13.611	-	6.045	6.908	-
	HSBT [56]	9.208	13.614	-	6.128	6.945	-
	Quasi-3D [42]	9.200	13.608	-	5.662	6.756	-
	Quasi-3D [40]	9.208	13.610	-	6.109	6.913	-
	Quasi-3D [5]	9.208	13.610	17.449	6.140	6.948	7.297
C-F	HSBT1	4.229	5.490	6.260	2.380	2.540	2.602
	HSBT2	4.242	5.492	6.259	2.386	2.542	2.602
	HSBT [4]	4.234	5.498	6.267	2.383	2.543	2.605
	HSBT [28]	4.230	5.491	-	2.378	2.541	-
	HSBT [56]	4.234	5.495	-	2.386	2.544	-
	Quasi-3D [40]	4.221	5.490	-	2.375	2.532	-
	Quasi-3D [5]	4.223	5.491	6.262	2.382	2.543	2.604
C-C	HSBT1	11.605	19.727	37.656	10.024	13.665	16.418
	HSBT2	11.607	19.823	37.666	10.169	13.741	16.424
	HSBT [4]	11.607	19.728	37.679	10.027	13.670	16.429
	HSBT [28]	11.602	19.719	-	10.011	13.657	-
	HSBT [56]	11.603	19.712	-	10.026	13.660	-
	Quasi-3D [40]	11.486	19.652	-	9.974	13.628	-
	Quasi-3D [5]	11.499	19.672	37.633	9.944	13.664	16.432

Table 8: Normalized fundamental frequencies of $[0^o/\theta^o/0^o]$ and $[0^o/\theta^o]$ composite beams (L/h=10, Materials I, E_1/E_2=40).

Lay-up	BC	Theory	Fibre angle						
			0^o	15^o	30^o	45^o	60^o	75^o	90^o
$0^o/\theta^o/0^o$	S-S	HSBT1	13.9946	13.8793	13.8102	13.7371	13.6701	13.6237	13.6071
		HSBT2	14.0035	13.8918	13.8209	13.7446	13.6743	13.6255	13.6081
		Quasi-3D [5]	13.9976	13.8822	13.8130	13.7400	13.6729	13.6264	13.6099
	C-F	HSBT1	5.6248	5.5610	5.5393	5.5205	5.5043	5.4934	5.4897
		HSBT2	5.6289	5.5825	5.5434	5.5243	5.5074	5.4961	5.4917
		Quasi-3D [5]	5.6259	5.5622	5.5403	5.5220	5.5059	5.4948	5.4909
	C-C	HSBT1	20.4944	20.4065	20.2490	20.0607	19.8761	19.7684	19.7267
		HSBT2	20.6114	20.5375	20.3568	20.1779	19.9946	19.8733	19.8227
		Quasi-3D [5]	20.4355	20.3428	20.1923	20.0062	19.8335	19.7144	19.6723
$0^o/\theta^o$	S-S	HSBT1	13.9946	10.0622	7.9727	7.2973	7.0498	6.9611	6.9401
		HSBT2	14.0035	10.0704	7.9812	7.3057	7.0582	6.9695	6.9485
		Quasi-3D [5]	13.9976	10.0656	7.9772	7.3028	7.0561	6.9682	6.9475
	C-F	HSBT1	5.6249	3.7978	2.9414	2.6771	2.5817	2.5481	2.5403
		HSBT2	5.6288	3.8002	2.9431	2.6785	2.5833	2.5497	2.5419
		Quasi-3D [5]	5.6259	3.7996	2.9428	2.6785	2.5837	2.5505	2.5428
	C-C	HSBT1	20.4933	17.4013	15.1143	14.2154	13.8432	13.6992	13.6646
		HSBT2	20.6263	17.4882	15.1665	14.2905	13.9232	13.7744	13.7408
		Quasi-3D [5]	20.4355	17.3592	15.0934	14.2004	13.8389	13.6989	13.6637

Table 9: Normalized buckling loads of ($0^o/90^o/0^o$) and ($0^o/90^o$) composite beams (Material I, E_1/E_2=40).

BC	Theory	$0^o/90^o/0^o$			$0^o/90^o$		
		5	10	50	5	10	50
S-S	HSBT1	8.609	18.814	30.859	3.902	4.935	5.398
	HSBT2	8.640	18.817	30.858	3.934	4.947	5.398
	HSBT [4]	8.613	18.832	30.906	3.907	4.942	5.406
	HSBT [56]	8.613	18.832	-	-	-	-
	Quasi-3D [40]	8.585	18.796	-	3.856	4.887	-
	Quasi-3D [5]	8.613	18.822	30.860	3.921	4.946	5.398
C-F	HSBT1	4.703	6.762	7.871	1.233	1.322	1.353
	HSBT2	4.703	6.760	7.880	1.236		
	HSBT [4]	4.708	6.772	7.886	1.236	1.324	1.356
	HSBT [56]	4.708	6.772	-	-	-	-
	Quasi-3D [40]	4.673	6.757	-	1.221	1.311	-
	Quasi-3D [5]	4.699	6.762	7.874	1.233	1.324	1.354
C-C	HSBT1	11.648	34.434	114.205	8.668	15.605	21.337
	HSBT2	11.710	34.556	113.530			
	HSBT [4]	11.652	34.453	114.398	8.674	15.626	21.372
	HSBT [56]	11.652	34.453	-	-	-	-
	Quasi-3D [40]	11.502	34.365	-	8.509	15.468	-
	Quasi-3D [5]	11.652	34.452	114.260	8.615	15.693	21.371

Table 10: Normalized buckling loads of $[0^o/\theta^o/0^o]$ and $[0^o/\theta^o]$ composite beams (L/h=10, Materials I, E_1/E_2=40).

Lay-up	Beam	Theory	Fibre angle						
			0^o	15^o	30^o	45^o	60^o	75^o	90^o
$0^o/\theta^o/0^o$	S-S	HSBT1	19.9039	19.5782	19.3830	19.1774	18.9896	18.8601	18.8141
		HSBT2	19.9294	19.6137	19.4133	19.1984	19.0013	18.8651	18.8167
		Quasi-3D [5]	19.9125	19.5865	19.3911	19.1853	18.9974	18.8677	18.821
	C-F	HSBT1	7.0626	6.8868	6.8409	6.8098	6.7838	6.7670	6.7615
		HSBT2	7.0652	6.8899	6.8429	6.8111	6.7855	6.7664	6.7599
		Quasi-3D [5]	7.0644	6.8878	6.8417	6.8111	6.7856	6.7683	6.7622
	C-C	HSBT1	37.0454	36.7878	36.2633	35.6056	34.9978	34.5808	34.4339
		HSBT2	37.2592	37.0212	36.5150	35.7803	35.1486	34.7106	34.5562
		Quasi-3D [5]	37.0660	36.8088	36.2838	35.6253	35.0169	34.5997	34.4524
$0^o/\theta^o$	S-S	HSBT1	19.9039	10.3304	6.5042	5.4539	5.0916	4.9647	4.9349
		HSBT2	19.9294	10.3475	6.5182	5.4665	5.1038	4.9768	4.9470
		Quasi-3D [5]	19.9125	10.3374	6.5116	5.4620	5.1007	4.9748	4.9455
	C-F	HSBT1	7.0637	3.0318	1.7834	1.4704	1.3658	1.3301	1.3219
		HSBT2	7.0653	3.0334	1.7844	1.4712	1.3667	1.3310	1.3227
		Quasi-3D [5]	7.0644	3.0334	1.7845	1.4714	1.3672	1.3317	1.3236
	C-C	HSBT1	37.0449	26.0773	19.2774	16.9307	16.0326	15.6903	15.6054
		HSBT2	37.2683	26.2200	19.4123	17.0623	16.1614	15.8146	15.7337
		Quasi-3D [5]	37.0660	26.1089	19.3221	16.9879	16.1028	15.7733	15.6927

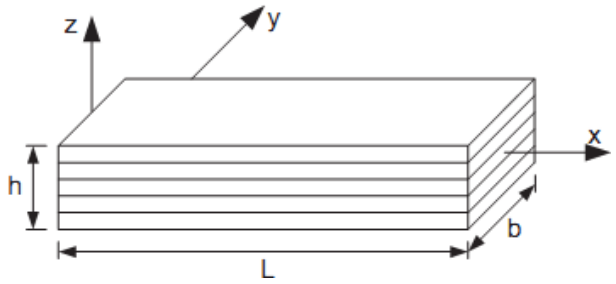

Figure 1: Geometric dimensions of a typical laminated composite beam.

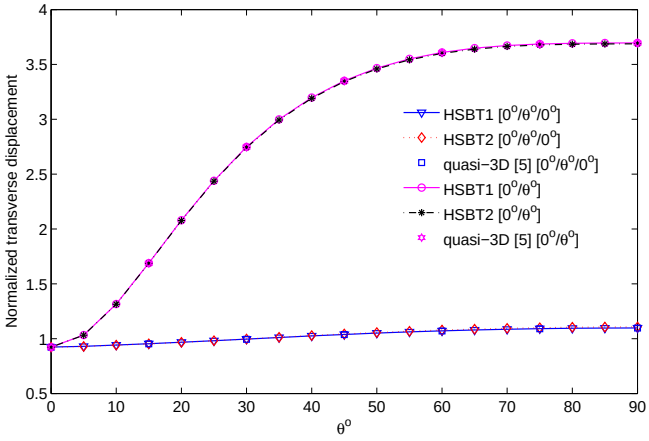

Figure 2: Influences of fibre orientation on normalized deflections of $[0^o/\theta^o/0^o]$ and $[0^o/\theta^o]$ composite beams under uniform loads (L/h=10, Material II, E_1/E_2=25).

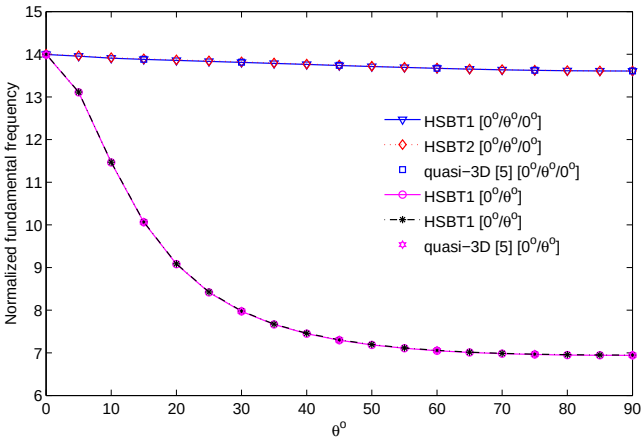

Figure 3: Influences of fibre orientation on normalized fundamental frequencies of $[0^o/\theta^o/0^o]$ and $[0^o/\theta^o]$ beams (L/h=10, Material I, E_1/E_2=40).

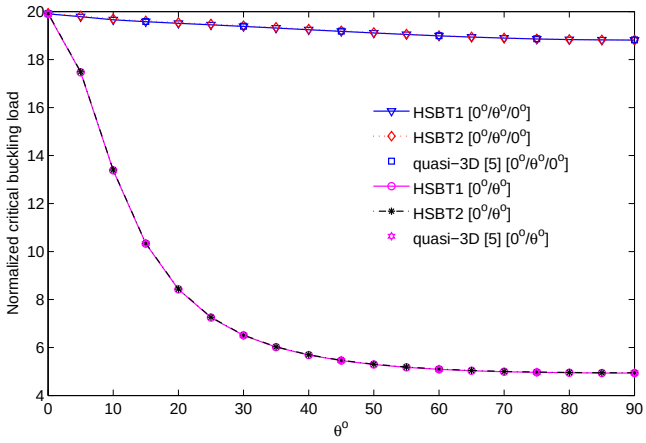

Figure 4: Influences of fibre orientation on normalized critical buckling loads of $[0^o/\theta^o/0^o]$ and $[0^o/\theta^o]$ beams (L/h=10, Material I, E_1/E_2=40).